12/17/2003

Weight-loss changes PPAR expression, reduces atherosclerosis and improves cardiovascular function in obese insulin-resistant mice

Wim Verreth[1], Peter Verhamme[1], Michel Pelat[2], Javier Ganame[3], John K. Bielicki[4], Ann Mertens[1], Rozenn Quarck[1], Nora Benhabilès[5], Gérard Marguerie[5], Bharti Mackness[6], Mike Mackness[6], Ewa Ninio[7], Marie-Christine Herregods[3], Jean-Luc Balligand[2], Paul Holvoet[1]

[1]Cardiovascular Research Unit of the Center for Experimental Surgery and Anesthesiology, Katholieke Universiteit Leuven, Belgium, [2]Department of Medicine, Unit of Pharmacology and Therapeutics, Université catholique de Louvain, Belgium, [3]Department of Cardiology, Katholieke Universiteit Leuven, Belgium; [4]Lawrence Berkeley National Laboratory, Berkeley, CA; [5] Clinigenetics, Nimes, France, [6]University of Manchester Department of Medicine, Manchester Royal Infirmary, Manchester, UK, [7]INSERM U525, Institut Fédératif CMV, Université Pierre et Marie Curie, Paris, France

Correspondence: Paul HOLVOET, PhD

Center for Experimental Surgery and Anesthesiology, Katholieke Universiteit Leuven, Herestraat 49, B-3000 Leuven, Belgium

Tel: 32-16-34.71.49

Fax: 32-16-34.71.14

E-mail: paul.holvoet@med.kuleuven.ac.be

ABSTRACT (Word count: 199)

Weight-loss in obese insulin-resistant, but not in insulin-sensitive, persons reduces CHD risk. It is not known to what extent changes in the adipose gene expression profile are important for reducing CHD risk. We studied the effect of diet restriction-induced weight-loss on gene expression in adipose tissue, atherosclerosis and cardiovascular function in mice with combined leptin and LDL-receptor deficiency. Obesity, hypertriglyceridemia and insulin-resistance are associated with hypertension, impaired left ventricle function and accelerated atherosclerosis in those mice. Diet restriction during 12 weeks caused a 45% weight-loss and changes in the gene expression in adipose tissue of PPARa and PPAR? and of key genes regulating glucose transport and insulin sensitivity, lipid metabolism, oxidative stress and inflammation, most of which are under the transcriptional control of PPARs. These changes were associated with increased insulin-sensitivity, decreased hypertriglyceridemia, reduced mean 24-hour blood pressure and heart rate, restored circadian variations of blood pressure and heart rate, increased ejection fraction, and reduced atherosclerosis. Thus, induction of PPARa and PPAR? in adipose tissue is a key mechanism for reducing atherosclerosis and improving cardiovascular function resulting from weight-loss. Our observations point to the critical role of PPARs in the pathogenesis of cardiovascular features of the metabolic syndrome.

Insulin resistance is now receiving increasing attention not only as a precursor to type 2 diabetes but also as a predictor of increased cardiovascular disease (1). Fat distributed in the abdominal region is a risk factor for type 2 diabetes and cardiovascular disease and is associated closely with insulin resistance (2). Weight-loss in insulin-resistant, but not in insulin-sensitive, obese persons reduces their CHD risk (3). It is however not known to what extent changes in the adipose gene expression profile are important for the association between abdominal fat, insulin resistance, hypertension, atherosclerosis and cardiac function (4).

We showed that mice with combined leptin and LDL-receptor deficiency (DKO) feature obesity, dyslipidemia, hypertension, insulin resistance and impaired glucose tolerance and/or diabetes. These metabolic syndrome attributes are associated with increased oxidative stress and accelerated atherosclerosis (5). Therefore we chose these mice to study the effect of weight-loss on hypertriglyceridemia, oxidative stress, hyperglycemia, hyperinsulinemia, hypertension, atherosclerosis and cardiovascular function. Because weight-loss in DKO mice was associated with reduced stigmata of cardiovascular risk, our second objective was to identify the underlying mechanisms.

Several adipokines have now been shown to regulate, directly or indirectly, a number of the processes that contribute to the development of atherosclerosis, including hypertension, endothelial dysfunction, insulin resistance, and vascular remodeling. Therefore we studied the effect of weight-loss on changes in the gene expression profiles in the intra-peritoneal adipose tissue that can explain changes in lipoprotein and lipid profile, oxidative stress, insulin sensitivity, glucose tolerance, blood pressure and heart rate regulation, and atherosclerosis.

METHODS

Experimental Protocol

Homozygous LDL-receptor knockout mice [LDLR(-/-)], heterozygous ob/+, and C57BL6 mice were purchased from Jackson Laboratory, Bar Harbor, ME. LDLR(-/-) mice were backcrossed into a C57BL6 background to the 10^{th} generation. To obtain DKO mice with combined leptin deficiency (ob/ob) and LDL-receptor deficiency, LDLR(-/-) and ob/+ mice were crossed as previously described (5). All offspring were genotyped by PCR techniques (6). All mice were housed at 22°C on a fixed 12/12-h light/dark cycle. Experimental procedures in animals were performed in accordance with protocols approved by the Institutional Animal Care and Research Advisory Committee.

All mice were fed standard chow, containing 4% of fat. Food intake of free-fed DKO mice was ~ 5.7g/day from weaning for 12, 24 or 36 weeks. Food intake of diet-restricted mice was restricted to 2.5g/day for 12 weeks between 12 and 24 weeks of age (24-week diet-restricted mice) or between 24 and 36 weeks of age (36-week diet-restricted mice) (Fig. 1). This amount corresponds to the daily intake of lean LDLR(-/-) mice.

Body Composition

Body composition was measured with PIXImus Mouse Densitometry (Lunar Corporation, Brussels) (7).

Microarray Analysis and Real Time RT-PCR

We performed 3 independent experiments with Agilent Mouse cDNA microarrays (product number: G4104A) that contain 9,600 clones among them 8,737 are unique and have a GenBank IDnumber. The source contents come from Incyte Mouse Unigene1 and the cDNA probe length lies between 500 and 1000bp. We compared the abundance of transcripts in two mRNA samples, one from the adipose tissue from a free-fed mouse, the other from a diet-restricted mouse. The sample preparation consisted of two rounds of amplification from total

RNA for dye swap hybridization. We used the cDNA labeling protocol recommended by Agilent (G2557 A kit) with the following modifications: 2.5 µg random hexamer primers (Invitrogen, at 3 µg/ µl) were added and 4 µg RNA for each microarray chip was used. The hybridization protocol recommended by Agilent was used according to kit G4104A. Slides were imaged using an Agilent scanner (Agilent G2565AA) with a resolution of 5 microns. Spot addressing, grid positioning, segmentation and intensity extraction (signal and background) were performed with Agilent Feature Extractor V.5.1.1 software (Agilent G2566AA Feature Extraction Software; Agilent Palo Alto, CA). Each spot was flagged according to 11 quality measures. In the general configuration, "spot Finder", "PolyOutlierFlagger" and "CoolieCutter" were retained. In Find Spot configuration, "Autofind corners" was selected with a "Dev Limit" of 70 microns. In CoolieCutter configuration, "Reject based on IQR" of 1.42 for feature and background was selected. In the PolyOutlierFlagger configuration, "Non-Uniformity Outlier Flagging" and "Population Outlier Flagging" were selected with the default. In order to correct print tip and intensity dependent effects, raw data were normalized in Clinigenetics according to a composite method based on dye-swap, print tip and scale normalization algorithms (8).

We also performed 2 experiments with Agilent mouse 60-mer microarrays to compare the expression of selected genes (Table 2) in free-fed and diet-restricted mice. More detailed microarray specifications can be downloaded from www.chem.agilent.com.

The level of mRNA expression for PPARα and PPARγ was also measured by real time RT-PCR. Total RNA was extracted from mouse adipose tissue using the Trizol reagent (InVitrogen, Life Technologies) and purified on a RNeasy kit column (Qiagen). First strand cDNA was generated from liver total RNA by reverse transcription using random primers from Takara and Superscript III reverse transcriptase (InVitrogen). Quantitative real time (RT) PCR was performed using Sybr®Green master mix according to the supplier protocols

(Applied Biosystems). Oligonucleotides (InVitrogen) used as forward primer (F) and reverse primer (R) were: for mouse *PPARa: F: 5'- TCAGGGTACCACTACGGAGTTCA -3'; R: 5'- CCGAATAGTTCGCCGAAAGA -3'*; for mouse *PPARg: F: 5'- GCAGCTACTGCATGTGATCAAGA -3'; R: 5'- GTCAGCGGGTGGGACTTTC -3'*; for mouse *b-actin: F: 5'- ACGGCCAGGTCATCACTATTG -3'; R: 5'- CACAGGATTCCATACCCAAGAAG -3'*. The level of mRNA expression for PPARα and PPARγ was calculated using the threshold cycle (C_t) value, *i.e.* the number of PCR cycles at which the fluorescent signal during the PCR reaches a fixed threshold. For each sample, both the C_t for the gene of interest and for the housekeeping gene β-actin were determined to calculate $\Delta C_{t,\text{sample}}$ ($C_{t,\text{target gene}} - C_{t,\text{housekeeping gene}}$), thus normalizing the data and correcting for differences in amount and/or quality between the different RNA samples. The expression levels were related to an external calibrator consisting of adipose tissue from C57BL6 control mice. Subsequently, $\Delta\Delta C_t$ ($\Delta C_{t,\text{sample}} - \Delta C_{t,\text{calibrator}}$) was determined, and the relative expression levels were calculated from $2^{-\Delta\Delta Ct}$, according to the manufacturer's instructions (Applied Biosystems). mRNA expression levels are, thus, indicated as arbitrary units ± SD (9).

Biochemical Analyses

Blood was collected into EDTA tubes after an overnight fast. Plasma was obtained by centrifugation, and lipoproteins were separated by FPLC (10). Protein levels were determined according to Bradford, free cholesterol and cholesterol ester levels by HPLC (11) and triglyceride levels with a diagnostic reagent kit (Sigma-Aldrich).

Glucose was measured with a glucometer (Menarini Diagnostics), plasma insulin with a mouse insulin ELISA (Mercodia), and adiponectin with a mouse adiponectin ELISA (Bio-Cat). Insulin resistance was calculated by a homeostasis model assessment (HOMA) = fasting serum insulin (mU/L) x fasting blood glucose (mmol/L)/22.5. To determine glucose tolerance,

glucose was measured in samples obtained by tail bleeding before and 15, 30, 60, 120 and 240 minutes after intra-peritoneal glucose administration (20% glucose solution; 2g/kg) (12).

Paraoxonase (PON), lecithin:cholesterol acyltransferase (LCAT) and PAF-acetylhydrolase (PAF-AH) activities were measured as previously described (13-15). The titers of Ig autoantibodies against oxidized LDL were determined in individual plasma samples (1:500 dilution). The amount of Ig bound to the MDA-LDL antigen was detected with alkaline phosphatase–labeled anti-mouse IgG. Data are expressed as relative absorbance units (RAU) (5).

Atherosclerosis

The extent of atherosclerosis was determined by analysis of cross-sections from the aortic root. Hearts were fixed in 4% phosphate-buffered formaldehyde and embedded in 25% gelatin. Approximately 10 7-μm frozen sections were used for morphometric and immunohistochemical analysis. Lipids were stained with oil-red O, oxidized LDL with mAb4E6, smooth muscle cells with an α-actin specific antibody (Dako), and macrophages with an antibody against mouse Mac-3 antigen (Pharmingen). Blinded analysis of positive immunostained sections was performed with the Quantimet600 image analyzer (Leica) (5).

Telemetry

BP signals, and HR, derived from pressure waves from the aortic arch, were measured in conscious, unrestrained animals with surgically implanted miniaturized telemetry devices (Datascience Corp, St Paul, MN, USA). This totally implantable system, allowing continuous recordings of BP and HR for several weeks, was surgically installed under general anesthesia, as described (16). After a week of recovery, short or long-term (24 hours), on-line recordings were digitized (range from 20- to 2000 Hz) and stored for further analysis.

Spectral analysis using a fast Fourier transformation algorithm on sequences of 512 points was performed by use of the HEM 3.4 software (Notocord systems) on BP and HR

recordings. The area under the curve was calculated for the very-low-frequency (VLF: 0.05 to 0.4 Hz), low-frequency (LF: 0.4 to 1.5 Hz), and high frequency (HF: 1.5 to 5.0 Hz) bands, as previously defined in the mouse species (17;18).

Echocardiography

Transthoracic echocardiography of 24-week free-fed and 24-week diet-restricted mice was performed with the use of a Philips SONOS 5500 with a 5-12 MHz ultraband cardiac phased probe (19). Mice were anesthetized with pentobarbital. The fractional area change, a measure for the ejection fraction (EF) was calculated from the LV cross-sectional area (2-D short axis) using the equation: EF (%) = ((LVDA – LVSA)/LVDA) x 100 where LVDA is the LV diastolic area and LVSA is the LV systolic area.

Statistical Analysis

Groups were compared Kruskal-Wallis test (Graph Pad Prism version 3.02) followed by Dunn's Multiple Comparisons test. A *P*-value of less than 0.05 was considered statistically significant.

RESULTS

Weight and Fat Mass

Figure 2A shows a 45 % weight-loss of 24-week diet-restricted mice compared to free-fed mice of the same age. Similar changes were observed in 36-week diet-restricted mice (Fig. 2A). The reduction of weight was due to a 33% loss of fat mass (Fig. 2B).

Adipose Tissue Gene Expression Profile and RT-PCR

Upon hybridization of fluorescent probes from the reverse transcribed RNA on cDNA chips (Agilent), 222 genes were significantly upregulated (mean ratio > 1.5) in the adipose tissue of diet-restricted mice and 114 genes were downregulated (ratio < 0.5) compared to free-fed mice. Table 1 shows the up-, respectively downregulated genes that are associated with adipocyte differentiation, glucose transport and insulin-sensitivity, hypertriglyceridemia, oxidative stress and inflammation.

Subsequently the Agilent mouse 60-mer microarray slides were used to confirm the data. The mean relative ratios (for 2 independent experiments) were 2.4 for PPARa, 3.1 for PPAR?, 4.9 for Ras, 2.7 for C/EBPa, 2.6 for FABP, 2.0 for angiotensinogen, 2.4 for LPL, 3.3 for VLDL receptor, 2.7 for hormone sensitive lipase, 2.7 for SOD-3, 2.5 for gluthathione peroxidase, and 4.6 for NOS-3.

Finally real time RT-PCR was performed to compare PPARα and PPARγ expression in adipose tissue from free fed and diet-restricted mice. The expression of PPARα was by 4.3-fold higher in the adipose tissue from diet-restricted mice (3.23±1.70 vs. 0.76±0.67 arbitrary units; n=6 per group; P=0.010). The expression of PPARγ was by 3.0-fold higher in the adipose tissue from diet-restricted mice (2.40±0.91 vs. 0.80±0.29 arbitrary units; n=8 per group; P=0.001).

Blood Analysis

Table 2 shows that weight-loss resulted in a 72% decrease of triglycerides, without changing total, non-HDL and HDL-cholesterol levels. HOMA for diet-restricted mice was 77% lower than that for free-fed mice (Fig. 2C). HOMA for diet-restricted mice was still 20-fold higher than that of lean mice (C57BL6 and LDL-receptor deficient mice). Linear regression analysis showed that weight-loss was responsible for 28% of the reduction in insulin, whereas the decrease in triglycerides was responsible for 55% of this reduction. A 12-week diet restriction resulted in a normalization of the glucose tolerance (Fig. 2D). The area under the curve for 24-week diet-restricted mice was similar to that of C57BL6 mice. Weight-loss resulted in an increase of plasma adiponectin from 29±8.6 (n=11) to 45±24 ng/ml (n=14; $P<0.05$).

PON activity, LCAT activity and Titer of Auto-immune Antibodies

Weight-loss was associated with a 1.7-fold increase in PON activity, a 1.6-fold increase of the LCAT activity, and a 1.5-fold decrease of the titer of Ig autoantibodies against oxidized LDL (Fig. 3). The LDL-associated PAF-AH was 1.3-fold lower in diet-restricted DKO mice; this difference was not significant.

Atherosclerosis

Figure 4 shows representative oil red O-stained sections of the aortic root from free-fed mice at 12, 24 and 36 weeks and from diet-restricted mice at 24 and 36 weeks. Lesions in the aortic root from 12-week free-fed mice were very small fatty streaks consisting of lipid-loaded macrophages. Plaque volumes increased from 0.005±0.003 mm^3 at 12 to 0.166±0.036 mm^3 at 24 and 0.302±0.101 mm^3 at 36 weeks. Plaque volumes in 24-week diet-restricted mice were 12-times smaller than in 24-week free-fed mice (Fig. 4). Plaque volumes in 36-week diet-restricted mice were similar to those in 24-week free-fed mice and 2.1–times smaller than in 36-week free-fed mice (Fig. 4). Lipid content of plaques in 36-week diet-restricted mice was only marginally lower than in 36-week free-fed mice. Macrophage content was 52% lower

and Ox-LDL content was 16% lower whereas smooth muscle content was 95% higher (Fig. 5).

Blood pressure, heart rate and ejection fraction

In control (C57BL6) mice, continuous (24 hours) BP and HR recordings revealed a typical variation during the light-dark cycle, i.e. light (corresponding to a resting period for mice) values of systolic (S) BP, diastolic (D) BP and HR were significantly lower than dark (activity period for mice) values. By contrast, circadian variations of HR and BP were totally abolished in free-fed DKO mice (Fig. 6A). These mice also had higher mean 24-hour SBP (128±1.3 vs. 112±1.3 mmHg, $p<0.05$) and DBP values (93±1.1 vs. 87 ±0.8 mmHg, $p<0.05$) and higher mean HR compared with controls (544±5.5 vs. 454 ±7.2 bpm, $p<0.05$). Twelve weeks diet restriction reduced all parameters in DKO mice to controls values (117.51 ± 1.8 mmHg, 87.8 ± 1.3mmHg and 402 ± 6.9 bpm, respectively). Figure 6A shows that diet restriction restored the circadian variations of SBP and HR in DKO mice.

Analysis of BP and HR variability of DKO mice revealed an increased variability of SBP in the Very Low Frequency domain (< 0.4 Hz, reflecting neurohumoral –including NO-influences), an increased variability of SBP in the Low Frequency domain (0.4-1.5 Hz, reflecting adrenergic tone), and, conversely, a decreased variability of HR in the High Frequency domain (above 1.5 Hz, reflecting vagal control). All these alterations were corrected in DKO mice submitted to diet restriction (Fig. 6 B).

Ejection fraction of C57BL6 mice was 51±6.2 %. At 24 weeks, ejection fraction of DKO mice was significantly lower (38±7.1 %; $P<0.01$). Diet restriction restored ejection fraction to 50±5.5 ($P<0.001$), a value comparable to that for C57BL6 mice (Fig. 6C).

DISCUSSION

Here we identified the up-regulation of both PPARa and PPAR? in adipose tissue as potentially important mechanisms to increase glucose transport and insulin-sensitivity, reduce hypertriglyceridemia, reduce oxidative stress and inflammation, to improve the hemodynamic situation and to inhibit atherosclerosis in leptin-deficient obese, insulin-resistant mice. These phenotypical changes were observed in the absence of leptin.

Both synthetic and natural ligands of PPAR? stimulate adipocyte differentiation that is associated with alleviation of insulin resistance presumably due to decreases in free fatty acids and up-regulation of adiponectin (20). They also improve glucose uptake in insulin-resistant tissues via an increase in the glucose transporter GLUT-4 (21;22). Analysis of gene expression of adipocytes of patients with insulin resistance showed a decreased adipocyte differentiation associated with decreased expression of PPARγ, adiponectin, FABP and LPL (23-25). Insulin-stimulated activation of MEK/ERK signaling promoted adipogenesis by enhancing C/EBPalpha and PPAR? gene expression during the differentiation of adipocytes (26). Insulin-stimulated PPAR? expression depended on the prenylation of the Ras family GTPases that assure normal phosphorylation and activation of CREB that, in turn, triggers the intrinsic cascade of adipogenesis by inducing the expression of GLUT-4 (27). Here we observed in association with increased PPAR gene expression, increased gene expression of Ras, GLUT-4, FABP, C/EBPalpha, and LPL in diet-restricted DKO mice. Plasma concentrations of adiponectin were higher in diet-restricted than in free-fed DKO mice that is in agreement with the recent finding in man that plasma adiponectin predicts insulin sensitivity of both glucose and lipid metabolism (28). Taken together all these changes support the increase in insulin sensitivity upon weight-loss. We observed increased expression of angiotensinogen in adipose tissue from diet-restricted mice. A local renin-angiotensinogen

system in human adipose tissue giving rise to angiotensin II (AngII), may act as a distinct system from that of the plasma system. Angiotensinogen mRNA and renin mRNA is most abundant in the adipocyte fraction of human adipose tissue. Angiotensin II stimulates the production and release of prostacyclin that, acting as an adipogenic hormone, promotes the differentiation of preadipocytes into adipocytes by activating all PPAR isoforms (for review (29;30)).

Reduction of triglyceride levels in diet-restricted DKO mice can be explained by increased expression of PPARa, lipoprotein lipase (LPL), the hormone-sensitive lipase and the VLDL receptor. In rodents, the central role of PPARa in fatty acid metabolism under feeding/fasting conditions has been clearly demonstrated. On severe fasting, PPARa activity and expression are induced, allowing the catabolism of fatty acids to produce ketone bodies, which serve as energy sources for extrahepatic tissues. In humans, pharmacological PPARa activation with fibrates decreases plasma triglyceride concentrations by increasing fatty acid uptake and catabolism, resulting in limited triglyceride and VLDL production by the liver (for review (31)). Lipoprotein lipase (LPL) catalyses the hydrolysis of triglycerides (32) and modulates the binding of TG-rich VLDL particles to the VLDL receptor (33). A defect in LPL can lead to hypertriglyceridemia and the development of atherosclerosis. On the other hand, LPL-induced lipolysis of triglyceride-rich lipoproteins generates PPARa ligands providing a link between lipoprotein metabolism and distal PPAR transcriptional effects (34). Lipid metabolism plays an important role in glucose homeostasis under normal and pathological conditions. A reduction in circulating or intracellular lipids by activation of PPARa improved insulin-sensitivity and the diabetic condition of mice (35). In adipocytes, skeletal muscle, and pancreatic ß-cells, lipids are mobilized from acylglycerides by the hormone-sensitive lipase

which deficiency results in a moderate impairment of insulin-sensitivity in multiple target tissues of the hormone but is compensated by hyperinsulinemia (36).

Oxidative stress is recognized as a key factor in atherogenesis (for review (37)). We have shown increased LDL oxidation in free-fed DKO mice (5) in agreement with increased levels of circulating oxidized LDL in obese persons without clinical evidence of cardiovascular disease (38;39). Here we show that weight-loss results in reduced oxidation of LDL that can be attributed to increased HDL-associated PON that is associated with lower cardiovascular risk (40). Decreased LDL oxidation in diet-restricted mice can also be due to the increased LCAT activity. We indeed showed that LCAT gene transfer in DKO mice inhibited LDL oxidation and prevented atherosclerosis (5). Weight-loss also resulted in lower expression of arachidonate-5-lipoxygenase that generates oxidized phospholipids in LDL that are mediators of coronary heart disease (41). Moreover it resulted in increased expression of superoxide dismutase and glutathione peroxidase. Decreased activity of these enzymes was associated with increased atherosclerosis (42). Finally, scavenger-receptor mediated uptake of oxidized LDL by macrophages results in foam cell formation. Platelet factor 4 enhanced the uptake of oxidized LDL by macrophages (43). Thus decreased expression of platelet factor 4 can result in decreased uptake of oxidized LDL and thus foam cell generation. The amount of oxidized LDL in the aortic arch from diet-restricted DKO mice was indeed lower than in free-fed mice.

Inflammation plays an important role in the development and the progression of atherosclerosis (for review (44)). Adipocytes also contribute to these processes (for review (44;45)). In vitro data, animal studies and some human studies suggest that PPAR agonists may not only regulate metabolic processes but may also limit inflammatory responses, including some involved in atherosclerosis (46;47). Indeed PPAR? activators inhibit the

expression of ICAM-1 in activated endothelial cells and reduce monocyte/macrophage homing to atherosclerotic plaques (48). We identified increased ICAM-1 expression and macrophage homing as an important mechanism of increased atherosclerosis in DKO mice (5). PPAR ? also suppresses thromboxane synthase gene transcription (49). We also observed decreased expression of CD22, CD44, CD53 and CD68. The latter is particularly interesting because it has been shown that the overexpression of the receptor for advanced glycation end products in diabetic $CD68^+$ macrophages is associated with enhanced inflammatory reaction. Expression of mast cell proteases that degrade HDL-associated apolipoproteins and thereby reduce its ability to promote cellular cholesterol efflux (50), was also decreased.

The increased variability of BP in free-fed DKO mice and the decrease of this variability upon weight-loss are potentially clinically important observations, given the adverse prognosis associated with increased SBP variability in humans (51). Our analysis of circadian variation of BP in unrestrained mice showed an elevated systolic and diastolic BP in free-fed DKO mice, and the absence of a physiologic "dip" of BP during the resting (daylight) period. Both anomalies recapitulate similar observations in human obesity-associated hypertension. The observed sympatho-vagal imbalance, with increased systolic BP variability in the Low Frequencies, reflects increased orthosympathetic activity. The decreased variability of HR in the High Frequency domain reflects impaired activity of the parasympathetic nervous system. This is further confirmed by the higher basal heart rate in free-fed DKO compared with control animals. The increased variability of SBP in the Very Low Frequency domain points to alterations of other neurohumoral control mechanisms of BP. Among these, we and others have shown that the nitric oxide synthase pathway is a major "buffering" system of systolic BP, and that chronic dyslipidemia specifically alters endothelial NO synthesis with a resultant increased variability of SBP (52;53). Our observation of *NOS3* up-regulation following diet

restriction in adipocyte tissue, if reflective of similar changes in the peripheral vasculature, would provide a strong mechanistic explanation for the improvement of endothelium and NO-dependent BP variability.

Conclusions: Inhibition of atherosclerosis and improvement of cardiovascular function following weight-loss in leptin-deficient, obese and insulin-resistant mice can be explained by expressional changes in the adipose tissue of key genes regulating oxidative stress, lipid metabolism and endothelial function, most of which are under the transcriptional control of PPARs. Our observation of increased expression of PPARs in the same condition points to the critical role of these transcription factors both in the pathogenesis and the potential treatment of these features of the metabolic syndrome.

ACKNOWLEDGEMENTS

This study is supported in part by the Fonds voor Wetenschappelijk Onderzoek–Vlaanderen (Program G.0263.01) and the Interuniversitaire Attractiepolen (Program 5/02). We thank Hilde Bernar, Els Deridder, Michèle Landeloos, and Dominique Stengel (INSERM U525) for excellent technical assistance.

Reference List

1. Haffner,S.M., Mykkanen,L., Festa,A., Burke,J.P., and Stern,M.P. 2000. Insulin-resistant prediabetic subjects have more atherogenic risk factors than insulin-sensitive prediabetic subjects: implications for preventing coronary heart disease during the prediabetic state. *Circulation* 101:975-980.

2. Abate,N., Garg,A., Peshock,R.M., Stray-Gundersen,J., and Grundy,S.M. 1995. Relationships of generalized and regional adiposity to insulin sensitivity in men. *J.Clin.Invest* 96:88-98.

3. McLaughlin,T., Abbasi,F., Kim,H.S., Lamendola,C., Schaaf,P., and Reaven,G. 2001. Relationship between insulin resistance, weight loss, and coronary heart disease risk in healthy, obese women. *Metabolism* 50:795-800.

4. Henkin,L., Bergman,R.N., Bowden,D.W., Ellsworth,D.L., Haffner,S.M., Langefeld,C.D., Mitchell,B.D., Norris,J.M., Rewers,M., Saad,M.F. *et al*. 2003. Genetic epidemiology of insulin resistance and visceral adiposity. The IRAS Family Study design and methods. *Ann.Epidemiol.* 13:211-217.

5. Mertens,A., Verhamme,P., Bielicki,J.K., Phillips,M.C., Quarck,R., Verreth,W., Stengel,D., Ninio,E., Navab,M., Mackness,B. *et al*. 2003. Increased low-density lipoprotein oxidation and impaired high-density lipoprotein antioxidant defense are associated with increased macrophage homing and atherosclerosis in dyslipidemic obese mice: LCAT gene transfer decreases atherosclerosis. *Circulation* 107:1640-1646.

6. Hasty,A.H., Shimano,H., Osuga,J., Namatame,I., Takahashi,A., Yahagi,N., Perrey,S., Iizuka,Y., Tamura,Y., Amemiya-Kudo,M. *et al*. 2001. Severe hypercholesterolemia, hypertriglyceridemia, and atherosclerosis in mice lacking both leptin and the low density lipoprotein receptor. *J.Biol.Chem.* 276:37402-37408.

7. Nagy,T.R. and Clair,A.L. 2000. Precision and accuracy of dual-energy X-ray absorptiometry for determining in vivo body composition of mice. *Obes.Res.* 8:392-398.

8. Yang,Y.H., Dudoit,S., Luu,P., Lin,D.M., Peng,V., Ngai,J., and Speed,T.P. 2002. Normalization for cDNA microarray data: a robust composite method addressing single and multiple slide systematic variation. *Nucleic Acids Res.* 30:e15.

9. Van Eck,M., Twisk,J., Hoekstra,M., Van Rij,B.T., Van der Lans,C.A., Bos,I.S., Kruijt,J.K., Kuipers,F., and Van Berkel,T.J. 2003. Differential effects of scavenger receptor BI deficiency on lipid metabolism in cells of the arterial wall and in the liver. *J.Biol.Chem.* 278:23699-23705.

10. Hedrick,C.C., Castellani,L.W., Warden,C.H., Puppione,D.L., and Lusis,A.J. 1993. Influence of mouse apolipoprotein A-II on plasma lipoproteins in transgenic mice. *J.Biol.Chem.* 268:20676-20682.

11. Vercaemst,R., Rosseneu,M., and Van Biervliet,J.P. 1983. Separation and quantitation of plasma lipoproteins by high-performance liquid chromatography. *J.Chromatogr.* 276:174-181.

12. Ludwig,D.S., Tritos,N.A., Mastaitis,J.W., Kulkarni,R., Kokkotou,E., Elmquist,J., Lowell,B., Flier,J.S., and Maratos-Flier,E. 2001. Melanin-concentrating hormone overexpression in transgenic mice leads to obesity and insulin resistance. *J.Clin.Invest* 107:379-386.

13. Bielicki,J.K. and Forte,T.M. 1999. Evidence that lipid hydroperoxides inhibit plasma lecithin:cholesterol acyltransferase activity. *J.Lipid Res.* 40:948-954.

14. Blankenberg,S., Stengel,D., Rupprecht,H.J., Bickel,C., Meyer,J., Cambien,F., Tiret,L., and Ninio,E. 2003. Plasma PAF-acetylhydrolase in patients with coronary artery disease: results of a cross-sectional analysis. *J.Lipid Res.* 44:1381-1386.

15. Mackness,M.I., Arrol,S., Abbott,C., and Durrington,P.N. 1993. Protection of low-density lipoprotein against oxidative modification by high-density lipoprotein associated paraoxonase. *Atherosclerosis* 104:129-135.

16. Butz,G.M. and Davisson,R.L. 2001. Long-term telemetric measurement of cardiovascular parameters in awake mice: a physiological genomics tool. *Physiol Genomics* 5:89-97.

17. Just,A., Faulhaber,J., and Ehmke,H. 2000. Autonomic cardiovascular control in conscious mice. *Am.J.Physiol Regul.Integr.Comp Physiol* 279:R2214-R2221.

18. Stauss,H.M., Stegmann,J.U., Persson,P.B., and Habler,H.J. 1999. Frequency response characteristics of sympathetic transmission to skin vascular smooth muscles in rats. *Am.J.Physiol* 277:R591-R600.

19. Yang,X.P., Liu,Y.H., Rhaleb,N.E., Kurihara,N., Kim,H.E., and Carretero,O.A. 1999. Echocardiographic assessment of cardiac function in conscious and anesthetized mice. *Am.J.Physiol* 277:H1967-H1974.

20. Yamauchi,T., Kamon,J., Waki,H., Murakami,K., Motojima,K., Komeda,K., Ide,T., Kubota,N., Terauchi,Y., Tobe,K. *et al*. 2001. The mechanisms by which both heterozygous peroxisome proliferator-activated receptor gamma (PPARgamma) deficiency and PPARgamma agonist improve insulin resistance. *J.Biol.Chem.* 276:41245-41254.

21. Komers,R. and Vrana,A. 1998. Thiazolidinediones--tools for the research of metabolic syndrome X. *Physiol Res.* 47:215-225.

22. Young,P.W., Cawthorne,M.A., Coyle,P.J., Holder,J.C., Holman,G.D., Kozka,I.J., Kirkham,D.M., Lister,C.A., and Smith,S.A. 1995. Repeat treatment of obese mice with BRL 49653, a new potent insulin sensitizer, enhances insulin action in white adipocytes. Association with increased insulin binding and cell-surface GLUT4 as measured by photoaffinity labeling. *Diabetes* 44:1087-1092.

23. Hensley,L.L., Ranganathan,G., Wagner,E.M., Wells,B.D., Daniel,J.C., Vu,D., Semenkovich,C.F., Zechner,R., and Kern,P.A. 2003. Transgenic mice expressing lipoprotein lipase in adipose tissue. Absence of the proximal 3'-untranslated region causes translational upregulation. *J.Biol.Chem.* 278:32702-32709.

24. Hong,G., Davis,B., Khatoon,N., Baker,S.F., and Brown,J. 2003. PPAR gamma-dependent anti-inflammatory action of rosiglitazone in human monocytes: suppression of TNF alpha secretion is not mediated by PTEN regulation. *Biochem.Biophys.Res.Commun.* 303:782-787.

25. Jansson,P.A., Pellme,F., Hammarstedt,A., Sandqvist,M., Brekke,H., Caidahl,K., Forsberg,M., Volkmann,R., Carvalho,E., Funahashi,T. *et al*. 2003. A novel cellular marker of insulin resistance and early atherosclerosis in humans is related to impaired fat cell differentiation and low adiponectin. *FASEB J.* 17:1434-1440.

26. Prusty,D., Park,B.H., Davis,K.E., and Farmer,S.R. 2002. Activation of MEK/ERK signaling promotes adipogenesis by enhancing peroxisome proliferator-activated receptor gamma (PPARgamma) and C/EBPalpha gene expression during the differentiation of 3T3-L1 preadipocytes. *J.Biol.Chem.* 277:46226-46232.

27. Klemm,D.J., Leitner,J.W., Watson,P., Nesterova,A., Reusch,J.E., Goalstone,M.L., and Draznin,B. 2001. Insulin-induced adipocyte differentiation. Activation of CREB rescues adipogenesis from the arrest caused by inhibition of prenylation. *J.Biol.Chem.* 276:28430-28435.

28. Tschritter,O., Fritsche,A., Thamer,C., Haap,M., Shirkavand,F., Rahe,S., Staiger,H., Maerker,E., Haring,H., and Stumvoll,M. 2003. Plasma adiponectin concentrations predict insulin sensitivity of both glucose and lipid metabolism. *Diabetes* 52:239-243.

29. Ailhaud,G. 1999. Cross talk between adipocytes and their precursors: relationships with adipose tissue development and blood pressure. *Ann.N.Y.Acad.Sci.* 892:127-133.

30. Engeli,S., Schling,P., Gorzelniak,K., Boschmann,M., Janke,J., Ailhaud,G., Teboul,M., Massiera,F., and Sharma,A.M. 2003. The adipose-tissue renin-angiotensin-aldosterone system: role in the metabolic syndrome? *Int.J.Biochem.Cell Biol.* 35:807-825.

31. Barbier,O., Torra,I.P., Duguay,Y., Blanquart,C., Fruchart,J.C., Glineur,C., and Staels,B. 2002. Pleiotropic actions of peroxisome proliferator-activated receptors in lipid metabolism and atherosclerosis. *Arterioscler.Thromb.Vasc.Biol.* 22:717-726.

32. Mead,J.R. and Ramji,D.P. 2002. The pivotal role of lipoprotein lipase in atherosclerosis. *Cardiovasc.Res.* 55:261-269.

33. Takahashi,S., Sakai,J., Fujino,T., Miyamori,I., and Yamamoto,T.T. 2003. The very low density lipoprotein (VLDL) receptor--a peripheral lipoprotein receptor for remnant lipoproteins into fatty acid active tissues. *Mol.Cell Biochem.* 248:121-127.

34. Ziouzenkova,O., Perrey,S., Asatryan,L., Hwang,J., MacNaul,K.L., Moller,D.E., Rader,D.J., Sevanian,A., Zechner,R., Hoefler,G. *et al*. 2003. Lipolysis of triglyceride-rich lipoproteins generates PPAR ligands: evidence for an antiinflammatory role for lipoprotein lipase. *Proc.Natl.Acad.Sci.U.S.A* 100:2730-2735.

35. Kim,H., Haluzik,M., Asghar,Z., Yau,D., Joseph,J.W., Fernandez,A.M., Reitman,M.L., Yakar,S., Stannard,B., Heron-Milhavet,L. *et al*. 2003. Peroxisome proliferator-activated receptor-alpha agonist treatment in a transgenic model of type 2 diabetes reverses the lipotoxic state and improves glucose homeostasis. *Diabetes* 52:1770-1778.

36. Mulder,H., Sorhede-Winzell,M., Contreras,J.A., Fex,M., Strom,K., Ploug,T., Galbo,H., Arner,P., Lundberg,C., Sundler,F. *et al*. 2003. Hormone-sensitive lipase null mice exhibit signs of impaired insulin sensitivity whereas insulin secretion is intact. *J.Biol.Chem.* 278:36380-36388.

37. Mertens,A. and Holvoet,P. 2001. Oxidized LDL and HDL: antagonists in atherothrombosis. *FASEB J.* 15:2073-2084.

38. Holvoet,P., Mertens,A., Verhamme,P., Bogaerts,K., Beyens,G., Verhaeghe,R., Collen,D., Muls,E., and Van de,W.F. 2001. Circulating oxidized LDL is a useful marker for identifying patients with coronary artery disease. *Arterioscler.Thromb.Vasc.Biol.* 21:844-848.

39. Holvoet,P., Harris,T.B., Tracy,R.P., Verhamme,P., Newman,A.B., Rubin,S.M., Simonsick,E.M., Colbert,L.H., and Kritchevsky,S.B. 2003. Association of High Coronary Heart Disease Risk Status With Circulating Oxidized LDL in the Well-Functioning Elderly: Findings From the Health, Aging, and Body Composition Study. *Arterioscler.Thromb.Vasc.Biol.* 23:1444-1448.

40. Mackness,B., Durrington,P., McElduff,P., Yarnell,J., Azam,N., Watt,M., and Mackness,M. 2003. Low paraoxonase activity predicts coronary events in the Caerphilly Prospective Study. *Circulation* 107:2775-2779.

41. Navab,M., Berliner,J.A., Subbanagounder,G., Hama,S., Lusis,A.J., Castellani,L.W., Reddy,S., Shih,D., Shi,W., Watson,A.D. *et al*. 2001. HDL and the inflammatory response induced by LDL-derived oxidized phospholipids. *Arterioscler.Thromb.Vasc.Biol.* 21:481-488.

42. 't Hoen,P.A., Van der Lans,C.A., Van Eck,M., Bijsterbosch,M.K., Van Berkel,T.J., and Twisk,J. 2003. Aorta of ApoE-deficient mice responds to atherogenic stimuli by a prelesional increase and subsequent decrease in the expression of antioxidant enzymes. *Circ.Res.* 93:262-269.

43. Nassar,T., Sachais,B.S., Akkawi,S., Kowalska,M.A., Bdeir,K., Leitersdorf,E., Hiss,E., Ziporen,L., Aviram,M., Cines,D. *et al*. 2003. Platelet factor 4 enhances the binding of oxidized low-density lipoprotein to vascular wall cells. *J.Biol.Chem.* 278:6187-6193.

44. Libby,P. 2002. Inflammation in atherosclerosis. *Nature* 420:868-874.

45. Rajala,M.W. and Scherer,P.E. 2003. Minireview: The adipocyte--at the crossroads of energy homeostasis, inflammation, and atherosclerosis. *Endocrinology* 144:3765-3773.

46. Hsueh,W.A. and Law,R. 2003. The central role of fat and effect of peroxisome proliferator-activated receptor-gamma on progression of insulin resistance and cardiovascular disease. *Am.J.Cardiol.* 92:3J-9J.

47. Plutzky,J. 2003. The potential role of peroxisome proliferator-activated receptors on inflammation in type 2 diabetes mellitus and atherosclerosis. *Am.J.Cardiol.* 92:34J-41J.

48. Pasceri,V., Wu,H.D., Willerson,J.T., and Yeh,E.T. 2000. Modulation of vascular inflammation in vitro and in vivo by peroxisome proliferator-activated receptor-gamma activators. *Circulation* 101:235-238.

49. Ikeda,Y., Sugawara,A., Taniyama,Y., Uruno,A., Igarashi,K., Arima,S., Ito,S., and Takeuchi,K. 2000. Suppression of rat thromboxane synthase gene transcription by peroxisome proliferator-activated receptor gamma in macrophages via an interaction with NRF2. *J.Biol.Chem.* 275:33142-33150.

50. Lee,M., Sommerhoff,C.P., von Eckardstein,A., Zettl,F., Fritz,H., and Kovanen,P.T. 2002. Mast cell tryptase degrades HDL and blocks its function as an acceptor of cellular cholesterol. *Arterioscler.Thromb.Vasc.Biol.* 22:2086-2091.

51. Sega,R., Corrao,G., Bombelli,M., Beltrame,L., Facchetti,R., Grassi,G., Ferrario,M., and Mancia,G. 2002. Blood pressure variability and organ damage in a general population: results from the PAMELA study (Pressioni Arteriose Monitorate E Loro Associazioni). *Hypertension* 39:710-714.

52. Pelat,M., Dessy,C., Massion,P., Desager,J.P., Feron,O., and Balligand,J.L. 2003. Rosuvastatin decreases caveolin-1 and improves nitric oxide-dependent heart rate and blood pressure variability in apolipoprotein E-/- mice in vivo. *Circulation* 107:2480-2486.

53. Stauss,H.M., Godecke,A., Mrowka,R., Schrader,J., and Persson,P.B. 1999. Enhanced blood pressure variability in eNOS knockout mice. *Hypertension* 33:1359-1363.

LEGENDS TO FIGURES

Figure 1: Experimental protocol. All mice were fed standard chow, containing 4% of fat. Food intake of free-fed DKO mice was ~ 5.7g/day. Food intake was restricted to 2.5g/day (black box) for 12 weeks between 12 and 24 weeks (24-week diet-restricted mice) or between 24 and 36 weeks (36-week diet-restricted mice).

Figure 2: (A) Weight loss 24-week diet-restricted, and 36-week diet-restricted DKO mice; (B) Fat mass in free-fed and diet-restricted DKO mice; (C) HOMA in free-fed and 24-week diet-restricted mice (similar changes were observed in 36-week diet-restricted mice); (D) Glucose tolerance in free-fed and diet-restricted mice. *P<0.05; **P<0.01.

Figure 3: Effect of diet restriction on PON (A) and LCAT (B) activity and on titer of Ig antibodies against oxidized LDL (C) that were measured as indicators of oxidative stress. *P<0.05; **P<0.01; ***P<0.001.

Figure 4: Representative cross-sections of the aortic arch from free-fed DKO mice at 12, 24 and 36 weeks, and from 24-week and 36-week diet-restricted mice. Plaque volumes in the aortic arch from 24- and 36-week free-fed and diet-restricted DKO mice. *P<0.05; **P<0.01; ***P<0.001.

Figure 5: Macrophage (A), oxidized LDL (B) and smooth muscle cell (SMC; C) content of plaques in the aortic arch from 36-week free-fed and diet-restricted mice. *P<0.05; **P<0.01; ***P<0.001.

Figure 6: (A) Circadian variations of systolic and diastolic BP and HR in C57BL6 control mice (?), and in free-fed (?) and diet-restricted (?) DKO mice. (B) Variation of systolic BP at very low frequency and at low frequency, and variation of HR at high frequency in C57BL6 control mice, and free-fed and diet-restricted DKO mice. (C) Ejection fraction of C57BL6 control mice, and free-fed and diet-restricted DKO mice. *P<0.05; **P<0.01.

Table 1: Gene expression in the adipose tissue from diet-restricted compared to free-fed DKO mice

ProbeName	GenBank Id	Unigene ID	Name	Exp. 1	Exp. 2	Exp. 3	Mean	SD
317536	W34083	Mm.3020	Peroxisome proliferator activated receptor gamma	2.0	0.9	4.0	**2.3**	1.6
1366165	AI020897	Mm.3903	Ras, dexamethasone-induced 1	3.8	4.6	4.9	**4.4**	0.6
935273	AA617613	Mm.2411	Ras-GTPase activating protein	2.5	1.6	2.1	**2.1**	0.5
517625	AA066475	Mm.10661	Solute carrier family 2 (facilitated glucose transporter), member 4	2.7	1.9	5.9	**3.5**	2.1
540533	AA161908	Mm.34537	CCAAT/enhancer binding protein (C/EBP), alpha	1.5	2.0	3.7	**2.4**	1.1
523460	AA080270	Mm.582	Fatty acid binding protein 4, adipocyte	1.0	1.7	2.8	**1.8**	0.9
987842	AA571053	Mm.8854	Angiotensinogen	1.8	2.8	2.0	**2.2**	0.5
620940	AA177240	Mm.12837	Nitric oxide synthase 3, endothelial cell	1.6	1.2	4.6	**2.5**	1.9
313176	W10495	Mm.1373	Peroxisome proliferator activated receptor alpha	1.5	1.6	2.4	**1.9**	0.5
1227378	AA739040	Mm.1514	Lipoprotein lipase	2.8	1.0	19	**7.81**	10
597754	AA154113	Mm.1721	Lipase, hormone sensitive	3.8	2.2	2.7	**2.9**	0.8

446084	AA020307	Mm.4141	Very low density lipoprotein receptor	1.3	1.2	4.5	**2.3**	1.9
1005832	AA606943	Mm.2400	Glutathione peroxidase 4	1.6	1.6	2.4	**1.8**	0.4
459497	AA027504	Mm.2407	Superoxide dismutase 3, extracellular	1.2	1.2	2.7	**1.7**	0.9
1383594	AI120986	Mm.23905	Platelet factor 4	0.3	0.2	0.6	**0.4**	0.2
1329349	AA930477	Mm.19844	Arachidonate 5-lipoxygenase activating protein	0.2	0.1	0.6	**0.3**	0.2
332372	W08586	Mm.28973	Intercellular adhesion molecule	0.4	0.5	0.5	**0.5**	0.1
1230835	AA880028	Mm.1708	CD22 antigen	0.5	0.5	0.2	**0.4**	0.2
642342	AA185112	Mm.200904	CD44 antigen	0.3	0.2	0.4	**0.3**	0.1
1020649	AA646061	Mm.2692	CD53 antigen	0.4	0.2	0.3	**0.3**	0.1
1263770	AA863715	Mm.15819	CD68 antigen	0.25	0.18	0.49	**0.31**	0.16
1381984	AA8332859	Mm.1252	Mast cell protease 5	0.08	0.09	0.16	**0.11**	0.04
314268	W10007	Mm.7409	Mast cell protease 6	0.16	0.2	0.31	**0.22**	0.08
1245329	AA821616	Mm.4054	Thromboxane A synthase-1, platelet	0.14	0.14	0.38	**0.22**	0.14

Table 2. Effect of diet restriction on blood parameters

	C57BL6	LDLR(-/-)	Ob/Ob	24-week Free-fed DKO	24-week Diet-restricted DKO
Total Cholesterol, mg/dL	78±19	213±68	136±51	537±276	446±200
Non-HDL-C, mg/dL	37±18	156±52	69±36	491±278	383±184
HDL-C, mg/dL	41±20	57±35	67±18	46±18	63±21
Triglycerides, mg/dL	23±5	65±20	29±7	596±293	130±6 *
Glucose, mmol/L	0.43±0.083	0.46±0.049	1.02±0.28	1.17±0.31	0.92±0.53
Insulin, mU/L	130±100	110±78	3190±580	3190±1110	930±440**

Data are means±SD for 10-12 mice per group. *P<0.05; **P<0.01. Data for 36-week free-fed and diet-restricted mice were very similar to those for 24-week free-fed, respectively diet-restricted mice.

Figure 1


Free-fed
2.5g/day
36-week Diet-restricted
36-week Free-fed
24-week Diet-restricted
24-week Free-fed
12-week Free-fed
Age (weeks)
Weaning
12
24
36

Figure 2

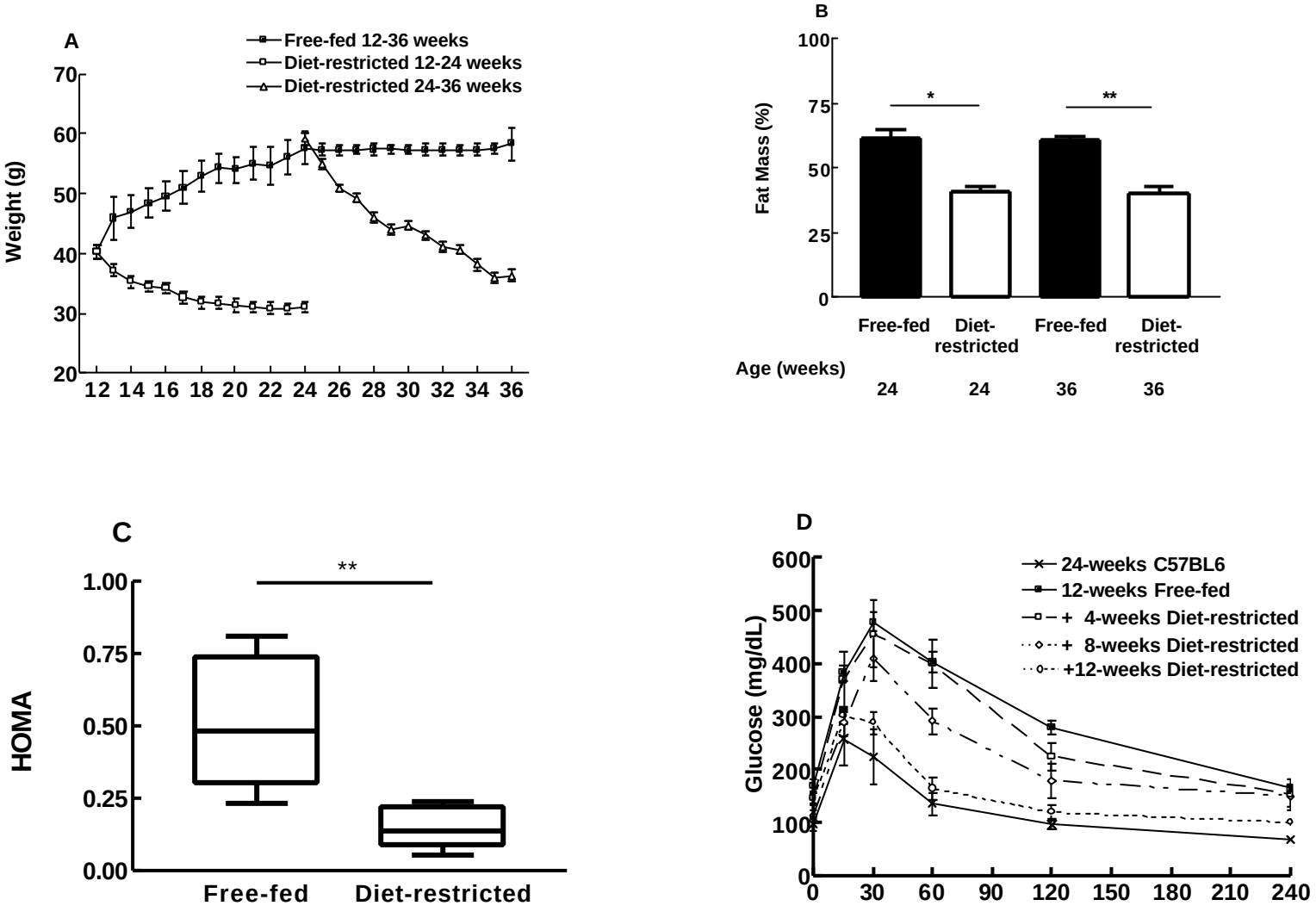
A
Free-fed 12-36 weeks
Diet-restricted 12-24 weeks
Diet-restricted 24-36 weeks
Weight (g)
70
60
50
40
30
20
12 14 16 18 20 22 24 26 28 30 32 34 36
B
100
75
50
25
0
Fat Mass (%)
*
**
Free-fed
Diet-restricted
Free-fed
Diet-restricted
Age (weeks)
24
24
36
36
C
**
1.00
0.75
0.50
0.25
0.00
HOMA
Free-fed
Diet-restricted
D
24-weeks C57BL6
12-weeks Free-fed
+ 4-weeks Diet-restricted
+ 8-weeks Diet-restricted
+12-weeks Diet-restricted
Glucose (mg/dL)
600
500
400
300
200
100
0
0 30 60 90 120 150 180 210 240

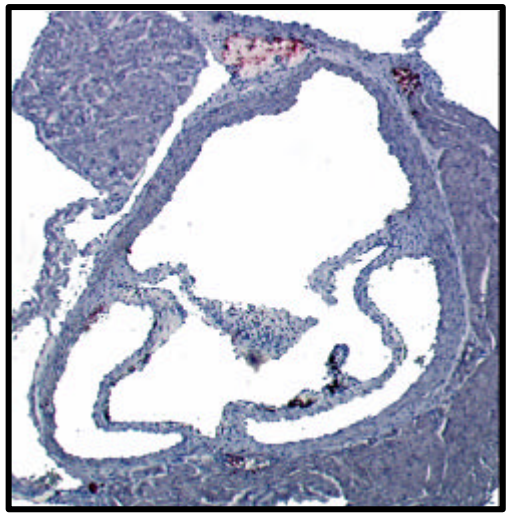

12-week Free-fed

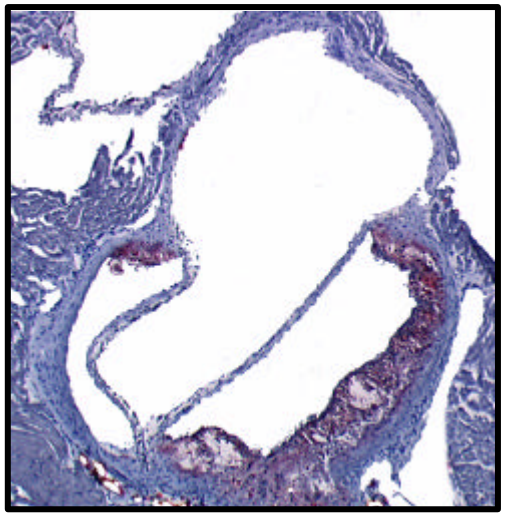

24-week Free-fed

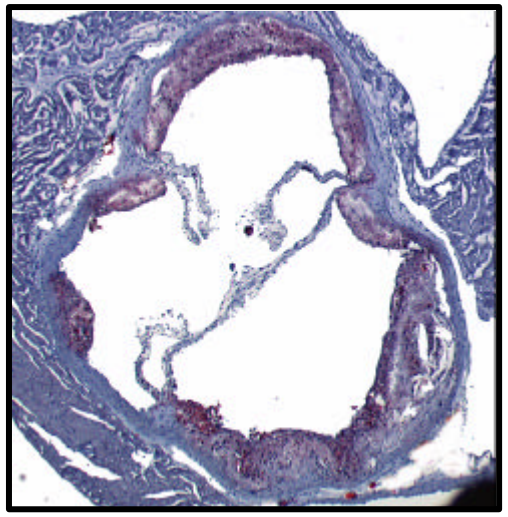

36-week Free-fed

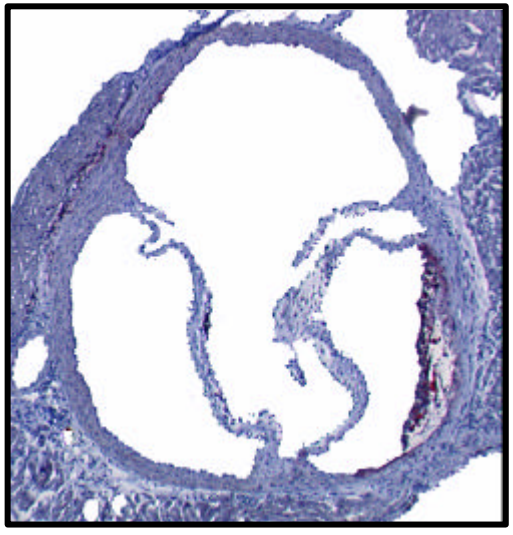

24- week Starved

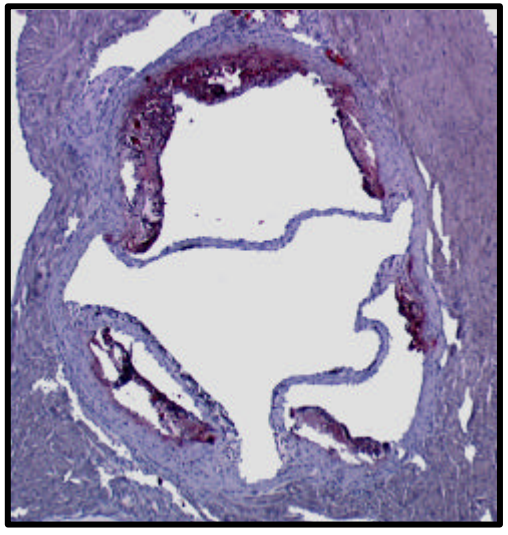

36-week Starved

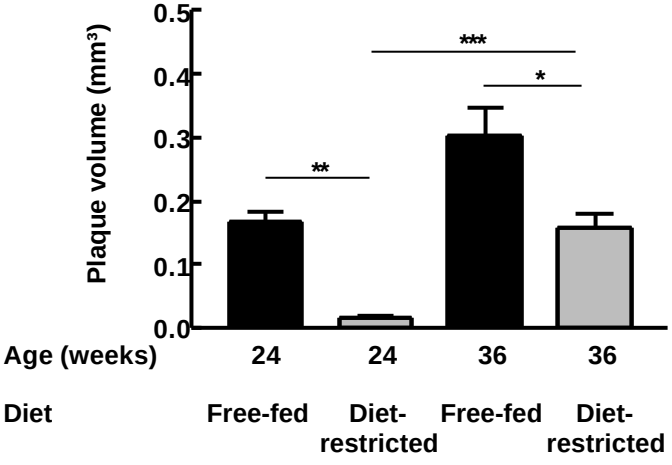

Figure 4

Figure 3

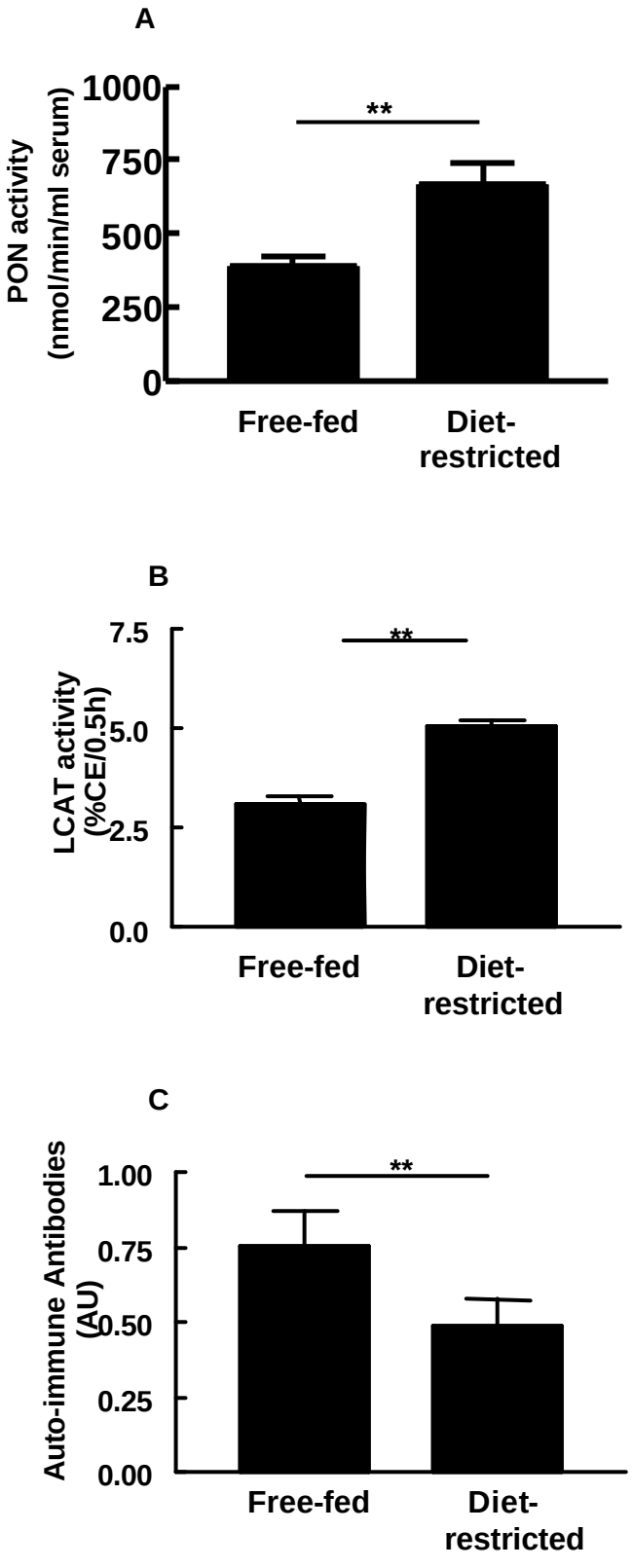
A
PON activity
(nmol/min/ml serum)
1000
750
500
250
0
**
Free-fed
Diet-
restricted
B
LCAT activity
(%CE/0.5h)
7.5
5.0
2.5
0.0
**
Free-fed
Diet-
restricted
C
Auto-immune Antibodies
(AU)
1.00
0.75
0.50
0.25
0.00
**
Free-fed
Diet-
restricted

Figure 5

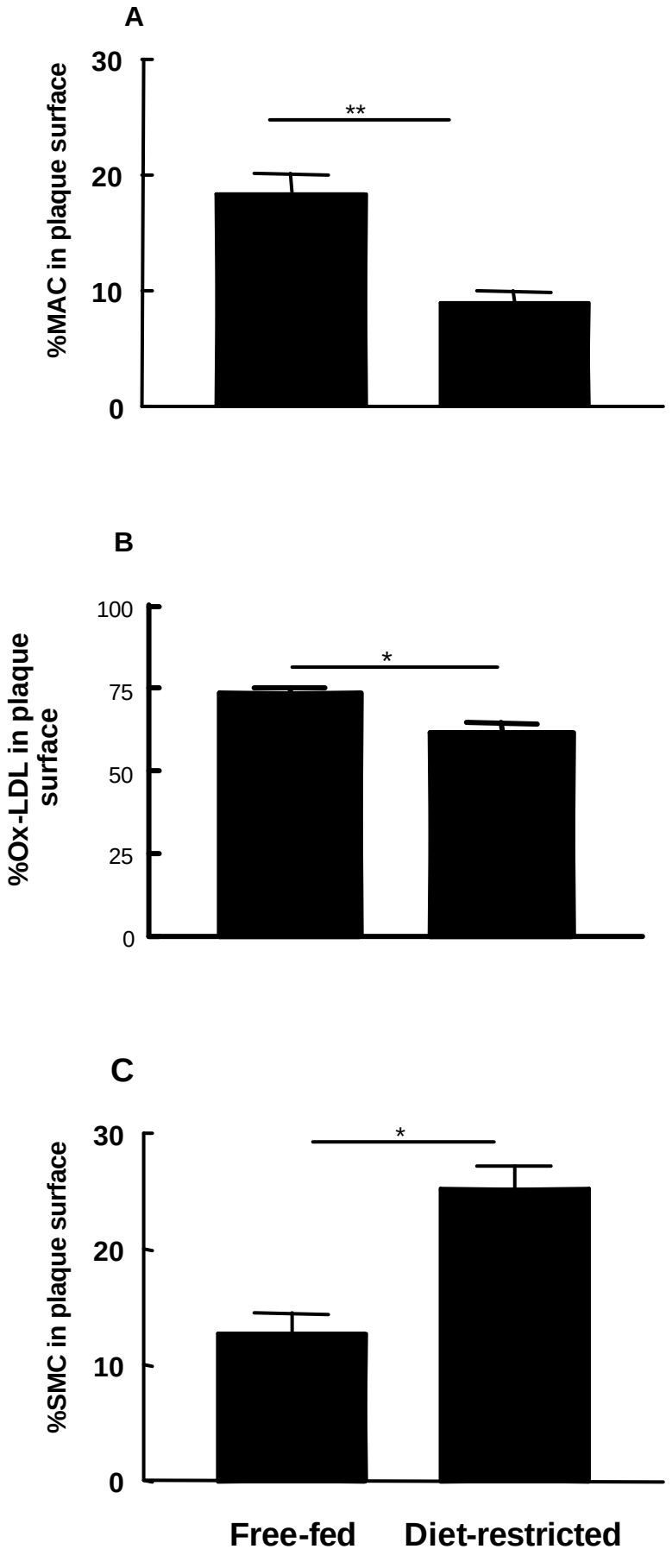
A
%MAC in plaque surface
30
20
10
0
**
B
%Ox-LDL in plaque surface
100
75
50
25
0
*
C
%SMC in plaque surface
30
20
10
0
*
Free-fed
Diet-restricted

Figure 6

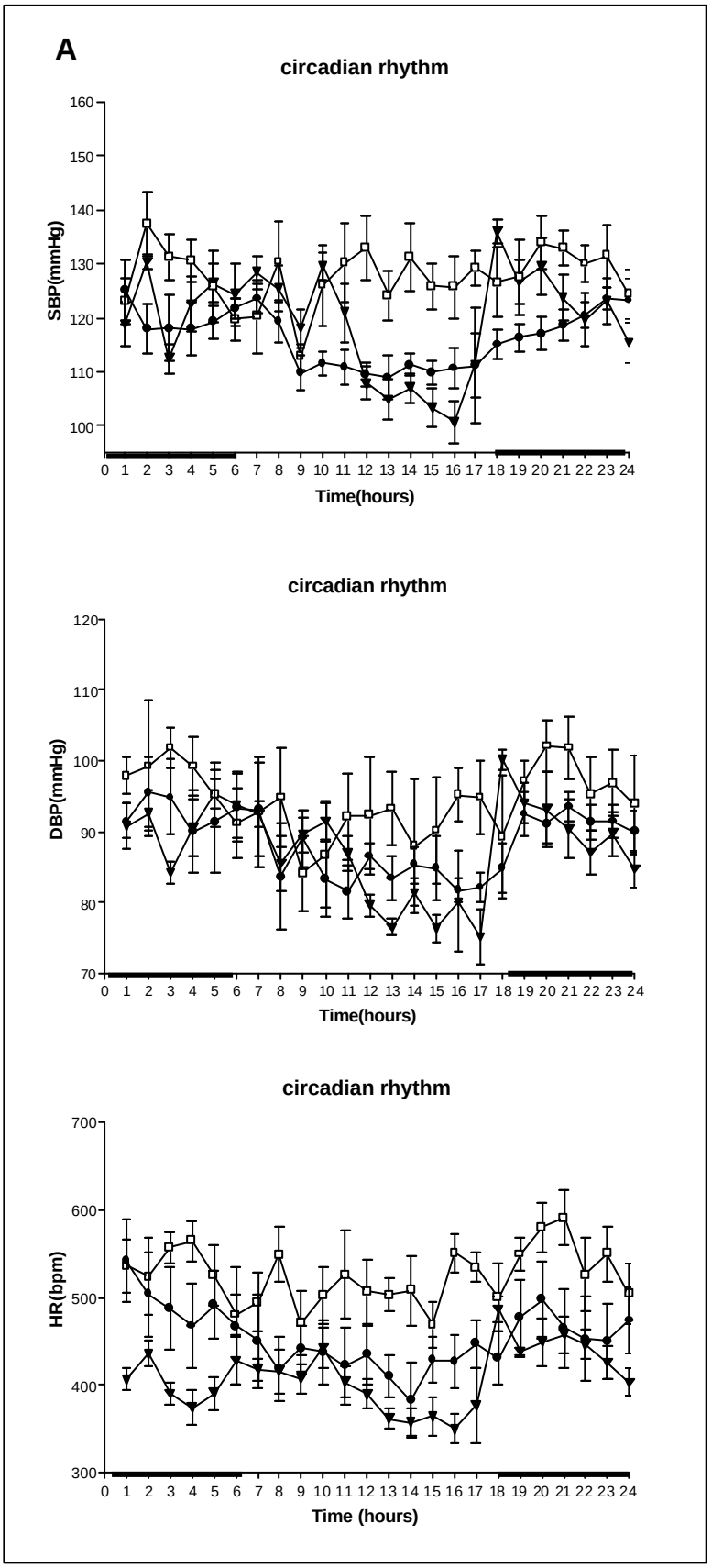
A
circadian rhythm
SBP(mmHg)
Time(hours)
circadian rhythm
DBP(mmHg)
Time(hours)
circadian rhythm
HR(bpm)
Time (hours)

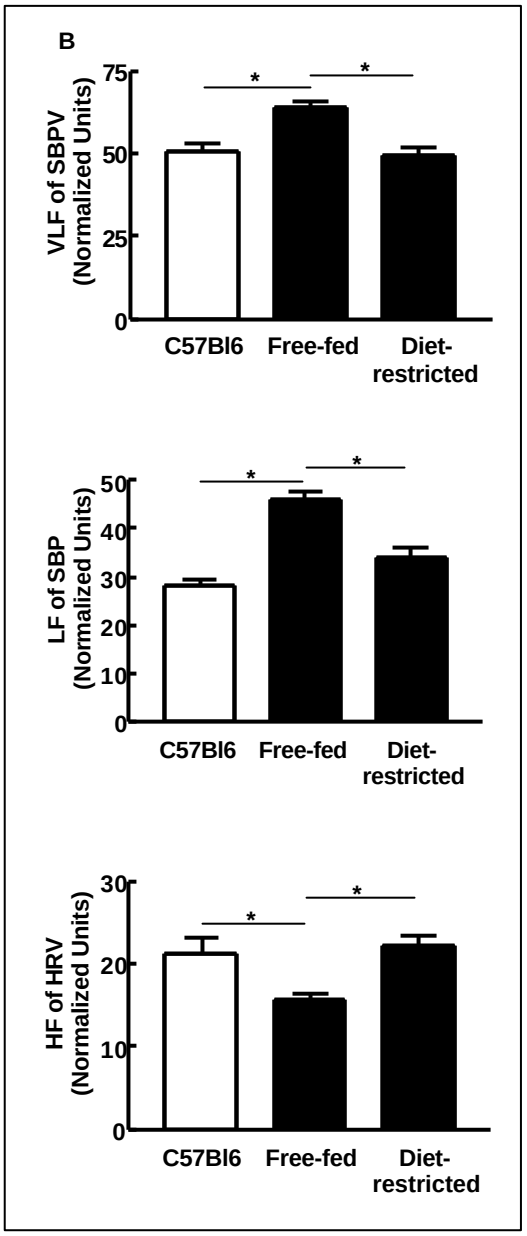
B
VLF of SBPV (Normalized Units)
C57Bl6
Free-fed
Diet-restricted
LF of SBP (Normalized Units)
HF of HRV (Normalized Units)

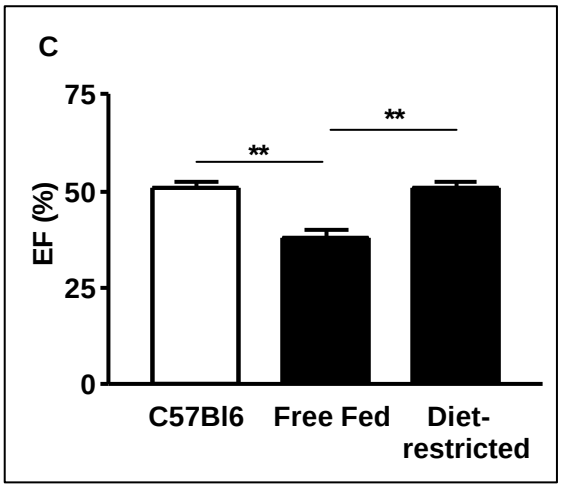
C
EF (%)
C57Bl6
Free Fed
Diet-restricted